

Application of Light Collecting Probe with High Spatial Resolution to Spark-Ignited Spherical Spray Flames

Young-Joon Yang*, Fumiteru Akamatsu, Masashi Katsuki

*Department of Mechanical Engineering, Osaka University,
2-1 Yamadaoka, Suita, Osaka 565-0871, Japan*

A light collecting probe named Multi-color Integrated Cassegrain Receiving Optics (MICRO) is applied to spark-ignited spherical spray flames to obtain the flame propagation speed in freely falling droplet suspension produced by an ultrasonic atomizer. Two MICRO probes are used to monitor time-series signals of OH chemiluminescence from two different locations in the flame. By detecting the arrival time difference of the propagating flame front, the flame propagation speed is calculated with a two-point delay-time method. In addition, time-series images of OH chemiluminescence are simultaneously obtained by a high-speed digital CCD camera to ensure the validity of the two-point delay-time method by the MICRO system. Furthermore, the relationship between the spray properties measured by phase Doppler anemometer (PDA) and the flame propagation speed are discussed with three different experimental conditions by changing the fuel injection rate. It was confirmed that the two-point delay-time method with two MICRO probes is useful and convenient to obtain the flame propagation speed and that the flame propagation speed depends on the spray properties.

Key Words : Light Collecting Probe, Chemiluminescence, Spray Combustion, Flame Propagation Speed

1. Introduction

Since liquid fuel spray flames are heterogeneous turbulent reacting two-phase flows, they have inherently complicated transient structures. Inhomogeneity of spray properties, such as number density, droplet size and velocity, is further complicated as the result of turbulent interactions, which produce various combustion phenomena in the same flow. It was reported that not only diffusion-mode phenomena but also premixed-mode behavior were observed in spray flames by Continillo and Sirignano (1990), Cessou and Stepowski (1996), Greenberg et al. (1996), Li and

Williams (1996), Chiu and Lin (1996), Gutheil and Sirignano (1998), and so on. Tsushima et al. (1998) concluded that some portions of the fuel spray disappear rapidly in a premixed-combustion-mode due to preferential flame propagation through easy-to-burn regions, whereas the non-flammable dense spray regions consist of droplet clusters surrounded by diffusion flames. The results suggest that spray flames do not behave as a conglomeration of single droplets but as a group or cluster of droplets with premixed and diffusion characteristics. Furthermore, in order to resolve the premixed-combustion-mode behavior in spray flames, clarification of the flame propagation mechanism and quantitative measurement of the flame propagation speed are strongly needed.

Akamatsu et al. (1994) observed a spark-ignited spherical flame propagating through a droplet suspension, which is freely falling and entraining surrounding air, in order to observe the flame

* Corresponding Author,

E-mail : yangj-du@hanmail.net

TEL : +82-51-200-6985; FAX : +82-51-200-7656

Department of Mechanical Engineering, Osaka University, 2-1 Yamadaoka, Suita, Osaka 565-0871, Japan.
(Manuscript Received May 18, 2004; Revised August 16, 2004)

propagation mechanism and the detailed flame structure in sprays under the minimal influences of atomization and fluid motion. In the study, a pair of short-exposure images of OH-radical chemiluminescence and either of flame luminosity in C₂-radical band or of Mie-scattering from droplet clusters were taken simultaneously to clarify the spatial relation between the nonluminous and luminous flames and unburned droplet clusters. Furthermore, this observation was compared with local continuous measurements, in which OH chemiluminescence, CH bands emission and droplet Mie scattering were simultaneously monitored together with the droplet sizes and velocities by phase Doppler anemometer (PDA). The research of Koo and Kim (2003) was referred to assess the technique of PDA. It was found that a nonluminous flame first propagated continuously through coexisting regions of small droplets and gas-phase mixture and that a number of small-scaled droplet clusters burned randomly associated with discontinuous luminous flames behind the nonluminous flame front.

In order to observe the flame propagation speed and the combustion characteristics in LPG and gasoline fuels, Lee et al. (2002) used the laser deflection method and high-speed Schlieren photography. The result concerning the flame propagation speed in this research shows that the laser deflection method has less than 5% error compared with that of high-speed camera.

In the present study, a pair of light collecting probe named the Multi-color Integrated Receiving Optics (MICRO) (Akamatsu et al. (1999)) is applied to the spark-ignited spherical spray flame for monitoring the time-series signals of OH chemiluminescence from two different locations separated at 6 mm in the vertical direction. The flame propagation speed is calculated by a two-point delay-time method, in which the time difference between onsets of two chemiluminescence signals detected by each MICRO probe can be measured. In addition, time-series images of OH chemiluminescence are simultaneously obtained by a high-speed digital CCD camera to ensure the validity of the two-point delay-time method with two MICRO probes. Furthermore, the relations-

hip between the spray properties measured by PDA and the flame propagation speed is investigated using three different fuel injection rates. It was confirmed that the two-point delay-time method using the two MICRO probes was very useful and accurate to obtain the flame propagation speed, and that the flame propagation speed were depending on the spray properties.

2. Experimental Apparatus

Figure 1 shows the experimental apparatus. A magnetostriction type ultrasonic atomizer (resonance frequency 18.5 kHz) located at 400 mm above a spark gap (4.0 mm) produces kerosene spray. The fuel injection rate was adjusted by an electrically-controlled microsyringe pump. A vertical square duct (280×280×1325 mm) was used to cover the whole test section in order to shield the droplet suspension from surrounding disturbances. The atomized droplets freely fall entraining surrounding air and were ignited by intermittent electric sparks at the gap. After the ignition, a spherical flame emerged near the spark gap and kept on growing with spherical shape for several tens of millisecond. Finally, the spherical

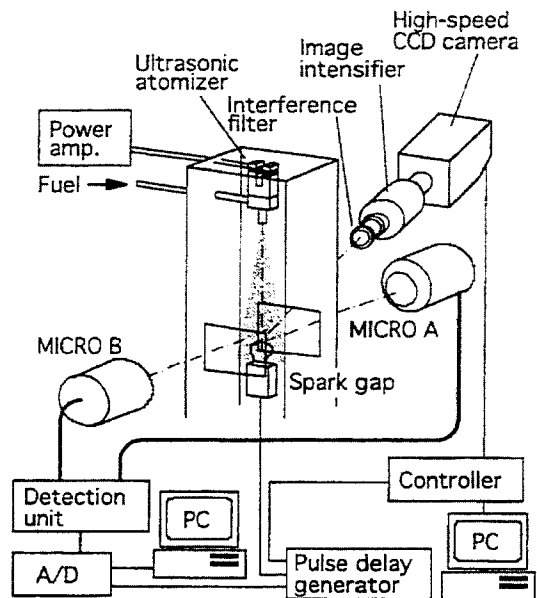


Fig. 1 Experimental apparatus

flame deformed flowing upward due to the buoyancy effect, and was extinguished by CO_2 injection just below the ultrasonic atomizer. Therefore, the observations were concentrated in the period of the spherical flame propagation. The experiments were conducted at three different fuel injection rates, 4.4, 6.3, and $11.0 \text{ cm}^3/\text{min}$. The ignition discharge duration time was 20 ms.

OH chemiluminescence represents the heat release rate of combustion reaction. The following reaction in hydrocarbon flames, $\text{CH} + \text{O}_2 = \text{OH}^* + \text{CO}$, is probably the main route to the formation of OH in the excited state. The OH is proportional to the concentration of CH. The process ${}^2\Sigma \rightarrow {}^2\Pi$ transition is occurred in about $1 \mu\text{s}$, leading to the emission of ultraviolet radiation at about 307 nm.

To detect OH radical chemiluminescence locally in the flame, two sets of light collecting probes named Multi-color Integrated Cassegrain Receiving Optics (MICRO) were used. Kauranen et al. (1990) and Nguyen and Paul (1996) have previously applied Cassegrain-type optics to combustion flows to monitor multi-color images.

Figure 2 shows the MICRO probe system used in this investigation, which consists of an optimized pair of concave and convex mirrors combined with an optical fiber cable (Mitsubishi Densen Co. Ltd., ST-U200D-SY, $\text{NA}=0.2$, core diameter= $200 \mu\text{m}$). The MICRO probe system had no chromatic aberration and minimized spherical aberration. In addition, the measurement volume center can be easily visualized using visible laser light guided into an optical fiber

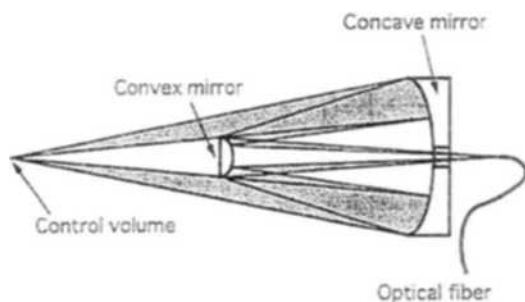


Fig. 2 Configuration of the Multi-color Integrated Cassegrain Receiving Optics (MICRO)

through a collimating lens (see Fig. 3) in the reverse direction. This feature enables precise optical alignment, which is necessary when dealing with UV signals, such as OH chemiluminescence. The light collection efficiency distribution of the system was evaluated using a ray-tracing method by Akamatsu et al. (1999), and the effective control volume size was estimated at 1.6 mm long and $200 \mu\text{m}$ in diameter.

The light collected by each MICRO probe was directed to a detection unit through the optical fiber cable, as shown in Fig. 3. The light emitted from the other end surface of the optical fiber cable expanded according to the numerical aperture (NA). To collimate the expanding light, a collimating lens was attached at the endsurface. The OH chemiluminescence signal in the collimated light was detected by photomultiplier tubes (Hamamatsu, R106UH) after passing through a narrow-band optical interference filter (peak wavelength= 308.5 nm , half-value width= 18 nm) to reject background noise. The current signals from the individual photomultiplier tubes (PMTs) were converted to voltage signals by I-V converters (NF Electronic Instrument, Model LI-76), amplified, and then filtered by an electrical low-pass frequency filter (NF Electronic, FV-665, cut-off-frequency= 5 kHz). The time-series signals were digitized into 12 bits, i.e. 0 to

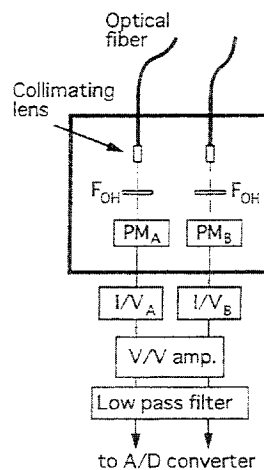


Fig. 3 Configuration of detection unit of the MICRO system

4096, by an A/D converter (Elmec, EC-2390) and recorded by a computer with digital sampling time of $10 \mu\text{s}$ (100 kHz).

Figure 4 shows the measurement location of two MICRO probes (MICRO A and MICRO B) and the spark gap. The MICRO A and B probes were aligned at 4 and 10 mm above the spark gap, respectively. The distance between the two measurement locations was 6 mm.

As shown in Fig. 3, to observe the evolving processes of the spherical spray flame, time-series images of OH chemiluminescence were recorded by a high-speed digital CCD camera (Kodak, EKTAPRO HS4540) simultaneously with the measurement of the two MICRO probes. The OH chemiluminescence from the flame was imaged onto a CCD array of 256×256 pixels in the high speed camera through an optical interference filter (peak wavelength = 308.5 nm, half-value width = 18 nm) and an image intensifier (Hamamatsu, C4273). Images were recorded in the transient memory of the image processing system and digitized into 8 bit, i.e. intensities between 0 and 255. The frame rate was 4,500 frames/s and the maximum number of frames obtained continuously in one run was limited to 1,024, which corresponds to the actual time of 228 ms due to the memory capacity of the image processor. A pulse-delay-generator (Stanford Research Systems, WC Model DG535) was used to control the triggering timing of the spark discharge and each measurement device.

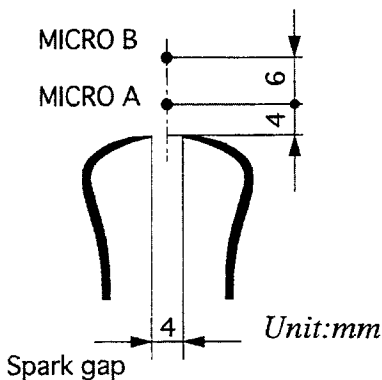


Fig. 4 Arrangement of measurement locations of two MICRO probes and the spark gap

3. Results and Discussion

3.1 Performance evaluation of the MICRO probe system

Before the MICRO probe system could be applied to the spherical spray flame, experimental verification of the MICRO system was conducted. Although the effective control volume size of the MICRO system was estimated at 1.6 mm long and $200 \mu\text{m}$ in diameter using the ray-tracing method, a fraction of the light emitted from outside the effective control volume does reach the detectors since chemiluminescence is spatially dispersed in flames and the MICRO system is designed for high sensitivity inside the effective control volume and not for completely blocking external signals. Therefore, simultaneous measurements of OH-radical chemiluminescence by the MICRO probe system and the ion current by an electro-static probe (Langmuir-probe), whose sensor tip is a Pt-Pt13%Rh thin wire of $100 \mu\text{m}$ in diameter and 1 mm long, were conducted in a premixed natural gas Bunsen flame. The inner diameter of the burner port is 11.4 mm. The flame appearance and the measurement point, which was 50 mm above from the burner port, are shown in Fig. 5. The measurement point is located at the fluctuating flame tip on the central axis of the flame.

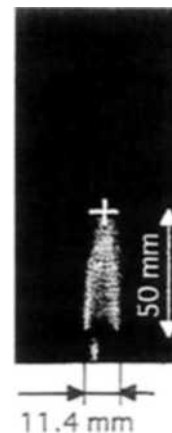


Fig. 5 A direct photograph of the premixed Bunsen flame with the measurement point of both the MICRO system and the electro-static probe

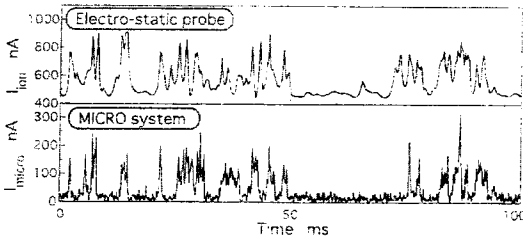


Fig. 6 Time-series signals of OH radical chemiluminescence obtained by the MICRO system and ion current detected by the electro-static probe

Figure 6 shows the simultaneous time-series signals of the ion current captured by the electro-static and OH radical chemiluminescence obtained by the MICRO system. The OH signals obtained by the MICRO probe show highly spatially resolved features equivalent to the ion current signals detected by the thin tip of the Langmuir probe. These results confirmed that the fraction of light collected from outside the effective control volume is negligible compared to the light collected inside the effective control volume. The MICRO probe system thus exhibited sufficiently high spatial resolution to observe local combustion phenomena without perturbing the flow.

3.2 Observation of growing processes of the spherical flame

Figure 7 shows time-series signals of OH-chemiluminescence, I_{OH} , obtained by the two MICRO probes together with the corresponding images of OH-chemiluminescence observed by the high-speed digital CCD camera. In image A at $t=0$ ms, when the spark ignition is initiated, the spark gap is superimposed. The white cross in each image shows measurement locations of each MICRO probe (see Fig. 4 for the detailed arrangement). As seen in these images, after the ignition, the flame front with low brightness is first propagating through the droplet cloud, and thereafter bright luminous lumps appear randomly inside the flame ball. The abrupt increase in time-series signal intensities of the MICRO A probe implies that the flame front passes through

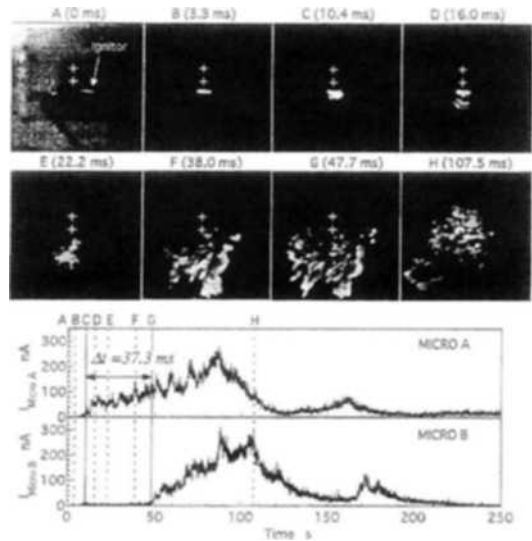


Fig. 7 Time-series data of OH chemiluminescence images recorded by the high speed CCD camera and local OH chemiluminescence monitored by the two MICRO systems

measurement location A at $t=10.4$ ms, while the MICRO B probe, focused at 6 mm above location A, detects the flame front at $t=47.7$ ms. Local chemiluminescence signals detected by the two MICRO probes are in good agreement with time-series OH chemiluminescence images observed by the high-speed digital CCD camera. Hence, the two-point delay-time method is adopted to deduce the flame propagation speed, V , which is defined as

$$V=L/\Delta t \quad (1)$$

where L denotes the distance between the two measurement locations, which corresponds to 6 mm in this experiment, and Δt is the time difference between the onset of the chemiluminescence signal detected by each MICRO probe. In the case shown in Fig. 5, the Δt is 37.3 ms. The flame propagation speed in this case is calculated at 0.16 m/s.

As reported by numerous researchers, such as Edwards et al. (1992), sprays have very inhomogeneous spatial and temporal structures such that statistical analysis is required for understanding spray flame behavior. In this study, the ignition tests were conducted approximately 100 times at

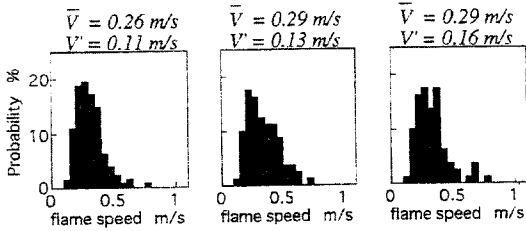

 (a) 4.4 cm³/min (b) 6.3 cm³/min (c) 11.0 cm³/min

Fig. 8 Probability distribution of the flame propagation speed

three different fuel injection rates, 4.4, 6.3, and 11.0 cm³/min.

Figure 8 shows the probability distribution of flame propagation speed obtained in each experimental condition. The average flame propagation speed, \bar{V} , measured in the three different conditions is almost the same, ranging from 0.26 m/s to 0.29 m/s, while the RMS value, V' , increases slightly with the fuel injection rate. This is explained by the increase in spray inhomogeneity with increased fuel injection rate, resulting in increased, non-uniform spatial and temporal flame propagation.

Since the droplets are freely falling with some velocity, the actual corrected flame propagation speed, V_c , in which downward droplet velocity is taken into account, should be deduced. Furthermore, spray characteristics are directly connected with flame structure. Hence, it is necessary to know spray properties such as mean diameter, size distribution, number density, slip velocities between gaseous phase and liquid phase and so on. In this study, PDA was applied to the freely falling droplets under isothermal conditions. The PDA control volume is located in the middle between the two measurement locations of the MICRO probes (7 mm above the spark gap). The droplet size distribution for the three different fuel injection rates are shown in Fig. 9, together with the Sauter mean diameter, D_{32} , mean velocity, \bar{U} , and RMS velocity, U' , of the freely falling droplets. It is shown that the Sauter mean diameter, the mean and RMS velocities increase with the fuel injection rate. The corrected actual flame propagation speed, V_c , is defined as follows,

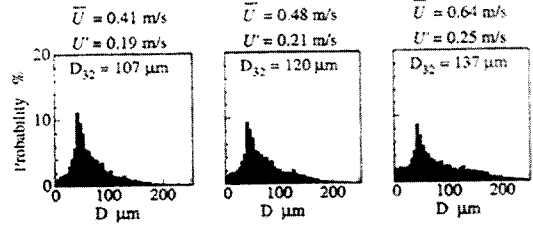
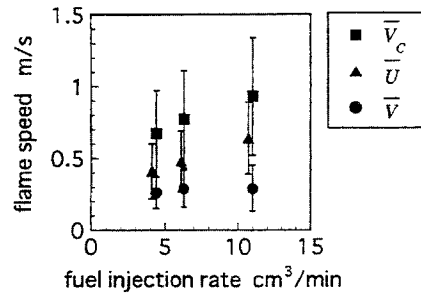

 (a) 4.4 cm³/min (b) 6.3 cm³/min (c) 11.0 cm³/min

Fig. 9 Size distribution of the droplet suspension at the three different fuel injection rate

Fig. 10 Variation of actual flame propagation speed at the three different fuel injection rate

$$V_c = V + \bar{U} \quad (2)$$

Figure 10 shows the variation of the corrected flame propagation speed, \bar{V}_c , in the three different fuel injection rates, together with the nominal flame propagation speed, \bar{V} , shown in Fig. 7, and the mean downward velocity of the freely falling droplets, \bar{U} , shown in Fig. 8. The solid circle, ●, indicates the average value, and the length of a line segment corresponds to the RMS value. It is shown that the actual corrected flame propagation speed, \bar{V}_c , gradually increases with the fuel injection rate. Increasing the fuel injection rate increases the mass of small droplets, which plays important role in flame propagation due to the increased evaporation rate of small droplets compared to larger droplets. Mizutani and Nakajima (1973) reported that flame propagation speed in their spray flame was enhanced by adding gaseous fuel at the optimized condition. Future work for this experiment is to identify the optimized fuel injection rate to enhance the flame propagation speed by conducting a number of experiments in various conditions.

4. Conclusions

In order to measure flame propagation speed in combusting spray systems, a pair of light collecting probes named the Multi-color Integrated Receiving Optics (MICRO) was applied to a spark-ignited spherical spray flame, propagation in a droplet suspension to monitor the time-series signals of OH chemiluminescence from two different locations.

(1) The performance of the MICRO probe was experimentally investigated in comparison with an electro-static probe (Langmuir-probe), with thin sensor tip. The results showed the MICRO probe has sufficiently high spatial resolution to observe local combustion reaction in flames without perturbing the flow.

(2) The flame propagation speed was calculated by a two-point delay-time method, in which the time difference between onsets of two chemiluminescence signals detected by each MICRO system was measured. In addition, time-series images of OH chemiluminescence were simultaneously obtained by a high-speed digital CCD camera to ensure the validity of the two-point delay-time method with two MICRO probes. It was demonstrated that the MICRO probe system was useful to observe time dependent phenomena such as flame propagation.

(3) The relationship between the spray properties measured by PDA and the flame propagation speed was investigated for three different fuel injection rates. As a result, the flame propagation speed was found to depend on the spray properties.

References

- Akamatsu, F., Nakabe, K., Katsuki, M., Mizutani, Y. and Tabata, T., 1994, "Structure of Spark-Ignited Spherical Flames Propagating in a Droplet Cloud," in *Developments in Laser Techniques and Applications to Fluid Mechanics*, Ed. R. J. Adrian, D. F. G. Durao, F. Durst, M. V. Heitor, M. Maeda, J. H. Whitelaw, pp. 212~223, Springer-Verlag.
- Akamatsu, F., Wakabayashi, T., Tsushima, S., Katsuki, M., Mizutani, Y., Ikeda, Y., Kawahara, N. and Nakajima, T., 1999, "Development of Light-Collecting Probe with High Spatial Resolution Applicable to Randomly Fluctuating Combustion Fields," *Measurement Science and Technology*, Vol. 10, pp. 1240~1246.
- Cessou, A. and Stepowski, D., 1996, "Planar Laser Induced Fluorescence Measurement of [OH] in the Stabilization Stage of a Spray Jet Flame," *Combust. Sci. and Tech.*, Vol. 118, pp. 361~381.
- Chiu, H. H. and Lin, C. L., 1996, "Anomalous Group Combustion of Premixed Clusters," *Proc. of the Combustion Institute*, Vol. 26, pp. 1653~1661.
- Continillo, G. and Sirignano, W. A., 1990, "Counterflow Spray Combustion Modeling," *Combust. Flame*, Vol. 81, pp. 325~340.
- Edwards, C. F. and Marx, K. D., 1992, "Analysis of the Ideal Phase-Doppler System: Limitations Imposed by the Single-Particle Constraint," *Atomization and Sprays*, Vol. 2, pp. 319~366.
- Greenberg, J. B., Silverman, I. and Tambour, Y., 1996, "A New Heterogeneous Burning Velocity Formula for the Propagation of a Laminar Flame Front Through a Polydisperse Spray of Droplets," *Combust. Flame*, Vol. 104, pp. 358~368.
- Gutheil, E. and Sirignano, W. A., 1998, "Counterflow Spray Combustion Modeling with Detailed Transport and Detailed Chemistry," *Combust. Flame*, Vol. 113, pp. 92~105.
- Kauranen, P. Andersson-Engles, S. and Svanberg, S., 1990, "Spatial Mapping of Flame Radical Emission Using a Spectroscopic Multi-Color Imaging System," *Appl. Phys.*, B53: pp. 260~264.
- Koo, J. Y. and Kim, J. H., 2003, "Assessment of a Phase Doppler Anemometry Technique in Dense Droplet Laden Jet," *KSME International Journal*, Vol. 17, No. 7, pp. 1083~1094 (in Korea).
- Lee, K. H., Lee, C. S., Ryu, J. D. and Choi, G.

M., 2002, "Analysis of Combustion and Flame Propagation Characteristics of LPG and Gasoline Fuels by Laser Deflection Method," *KSME International Journal*, Vol. 16, No. 7, pp. 935~941.

Li, S. C. and Williams, F. A., 1996, "Experimental and Numerical Studies of Two-Stage Methanol Flames," *Proc. of the Combustion Institute*, Vol. 26, pp. 1017~1024.

Mizutani, Y. and Nakajima, A., 1973, "Combustion of Fuel Vapor-drop-air Systems," *Combust. Flame*, Vol. 21, pp. 343~357.

Nguyen, Q. V. and Paul, P. H., 1996, "The Time Evolution of a Vortex-Flame Interaction Observed via Planar Imaging of CH and OH," *Proc. of the Combustion Institute*, Vol. 26, pp. 357~364.

Tsushima, S., Saitoh, H., Akamatsu, F. and Katsuki, M., 1998, "Observation of Combustion Characteristics of Droplet Clusters in a Premixed-Spray Flame by Simultaneous Monitoring of Planar Spray Images and Local Chemiluminescence," *Proc. of the Combustion Institute*, Vol. 27, pp. 1967~1974.